Biochem. J. (1992) 281, 795–802 (Printed in Great Britain)

Kinetics of superoxide scavenging by dismutase enzymes and manganese mimics determined by electron spin resonance

Brian GRAY* and Alasdair J. CARMICHAEL†‡

*Radiation Biochemistry Department and †Radiation Biophysics Department, Armed Forces Radiobiology Research Institute, Bethesda, MD 20889-5145, U.S.A.

This study presents an e.s.r. assay for superoxide dismutase (SOD). Enzymic reactions were studied in which Cu,Zn-SOD, Mn-SOD and Fe-SOD each competed with the spin trap 5,5-dimethyl-1-pyrroline 1-oxide (DMPO) for superoxide anion (O_2^-) at pH 7.8. O_2^- from dissolved KO_2 (potassium superoxide) in dimethyl sulphoxide was added directly to the enzyme solutions containing DMPO. The results show that, in this competition reaction system, the kinetics of the reactions between the enzymes and O_2^- follow a function $y = f([SOD]^{0.5})$. The rate constant, $k_{SOD} = 6.4 \times 10^9$ M$^{-1}\cdot$S^{-1}, determined for Cu,Zn-SOD is approximately an order of magnitude larger than those for Mn-SOD and Fe-SOD. A comparative study of reported SOD mimics, including Mn^{2+}, MnO_2–desferrioxamine mesylate (Desferal) and MnO_2–Desferal–ascorbate, was done. The results show that solutions of these complexes are approximately three orders of magnitude less active than Cu,Zn-SOD and approximately two orders of magnitude less active than Mn-SOD or Fe-SOD. The results also suggest that the reactivity toward O_2^- in solutions of these complexes originates from the Mn^{2+} present and not from the MnO_2–Desferal complexes.

INTRODUCTION

Enzymes catalysing the dismutation of superoxide anion (O_2^-) have been isolated, characterized and discussed in various papers and reviews [1–6]. These superoxide dismutase (SOD) enzymes contain metal ions which are cyclically reduced and oxidized during catalysis [7–9]. Although exact details of the catalytic mechanism are still under investigation, the cyclic redox reactions of the metals as shown in reactions (1) and (2) are generally accepted [10]:

$$M^{n+}\cdot SOD + O_2^- \rightleftharpoons [M^{n+}\cdot SOD - O_2^-] \rightleftharpoons M^{(n-1)+}\cdot SOD + O_2 \quad (1)$$

$$M^{(n-1)+}\cdot SOD + O_2^- + 2H^+ \rightleftharpoons [M^{(n-1)+}\cdot SOD - O_2H_2] \rightleftharpoons M^{n+}\cdot SOD + H_2O_2 \quad (2)$$

Two of the three types of metal-containing enzymes, Cu,Zn-SOD and Fe-SOD, have been studied by stopped-flow techniques, and the resultant data fit the Michaelis–Menten steady-state kinetic model [11–13]. Steady-state assumptions provide the rationale for many competition kinetic assays developed for reactions having transient free radicals as substrates [14,15]. The present paper reports results of competition-kinetic studies of SOD enzymes and of manganese-containing preparations that are reportedly mimics of SOD enzymes.

Competition assays for O_2^- dismutase activity in aqueous solutions have a background spontaneous dismutation reaction occurring (reaction 3):

$$2H^+ + 2O_2^- \rightarrow H_2O_2 + O_2 \quad (3)$$

The rate constant for this reaction is approx. 2×10^5 M$^{-1}\cdot$s^{-1} at pH 7.8 [16]. Any detector molecule must compete for O_2^- against this spontaneous dismutation background reaction plus dismutase enzymes or mimics present in reaction solutions. 5,5-Dimethyl-1-pyrroline 1-oxide (DMPO) reacts with O_2^- forming the DMPO–O_2^- spin adduct radical through the bimolecular mechanism shown in reaction (4) [17]:

$$O_2^- + DMPO \rightarrow DMPO\text{–}O_2^- \quad (4)$$

The calculated rate constant (k_{DMPO}) for reaction (4) is about 18 M$^{-1}\cdot$s^{-1} at pH 7.8, and the spin adduct formed is sufficiently stable for quantification by e.s.r. [18,19]. It is known that O_2^- reacts with both of the spin adducts: DMPO–O_2^- and the decomposition product, DMPO–OH, formed from DMPO–O_2^- [20,21]. The products of these reactions with O_2^- are e.s.r.-silent. The rates of each reaction depend on the concentrations of DMPO–O_2^-, DMPO–OH and the O_2^- concentration. Therefore, competition experiments using DMPO as a detector should rely on an initial introduction of O_2^- rather than a steady-state flux of O_2^- generated continuously to minimize formation of e.s.r.-silent products. Also, it must be demonstrated that the combined DMPO–O_2^- and DMPO–OH e.s.r. signal varies with the logarithm of the SOD concentration. This insures that spontaneous dismutation plus scavenging by DMPO–O_2^- and DMPO–OH are not masking O_2^- removal by SOD, permitting the use of DMPO as a detector molecule in competition assays over a limited range centred around the equality shown in eqn. (A):

$$k_{DMPO}[DMPO][O_2^-] = k_{SOD}[SOD][O_2^-] \quad (A)$$

Reactions (1) and (2) combined have the overall rate constant k_{SOD}. The comparatively low k_{DMPO} value permits competition assays for relatively small SOD concentrations, since k_{SOD} values approach rate constants for diffusion-controlled reactions [7,22,23].

A dismutase assay based on competition between SOD and DMPO for O_2^- has been described [19]. The assay used a xanthine–xanthine oxidase O_2^--generating system rather than an initial introduction of potassium superoxide (KO_2) as described in the present study. The decrease in DMPO–O_2^--spin-adduct concentration was measured at various SOD concentrations and found to be a logarithmic function of the enzyme concentration. The concentration of SOD that reduced the DMPO–O_2^- spin adduct concentration by 50% (ID_{50}) was determined, and eqn. (A) was used to calculate k_{SOD} values for Cu,Zn-SOD, Fe-SOD, Mn-SOD, and additional O_2^- scavengers.

Abbreviations used: SOD, superoxide dismutase; O_2^-, superoxide (anion); DMPO, 5,5-dimethyl-1-pyrroline 1-oxide; DMSO, dimethyl sulphoxide; ID_{50}, concentration of SOD that reduced the DMPO–O_2^--spin-adduct concentration by 50%; Desferal, desferrioxamine mesylate; KO_2, potassium superoxide.

‡ To whom correspondence should be sent.

The search for low-molecular-mass SOD mimics has been extensive, because such compounds could augment endogenous cellular enzyme levels [24–28]. Recently, Mn complexes of desferrioxamine mesylate (Desferal) have been prepared and examined for SOD-enzyme-mimetic activity [29,30]. Two of these Mn–Desferal complexes appear to have O_2^--dismutation activities equal or superior to Mn^{2+} when assayed by the cytochrome *c* competition assay [31]. However, EDTA eliminated the O_2^- dismutase activity of each complex and that of Mn^{2+} [31,32]. In addition, there are numerous subtle artifacts that may undermine attempts to assay dismutase activities of metals or metal complexes by the cytochrome *c* assay method [33]. First, oxidized cytochrome *c* may be reduced directly by the metal or metal complexes [34,35]. Conversely, reduced cytochrome *c* may be oxidized by the metal or metal complexes [36,37]. Also, the test compound may inhibit the enzymic production of O_2^- by the xanthine–xanthine oxidase generating system. Finally, rapid reoxidation of the reduced metal intermediate by molecular oxygen (reversal of reaction 1) must be considered in assays generating a low steady-state concentration of O_2^- [33]. These problems have led to numerous attempts to develop an alternative method for determining SOD activity. The present paper reports the utilization of an e.s.r. method based on competition for O_2^- between DMPO and authentic SOD enzymes or suspected mimics.

EXPERIMENTAL

Bovine erythrocyte Cu,Zn-SOD, *Escherichia coli* Mn-SOD and Fe-SOD, Desferal, horse heart cytochrome *c*, xanthine, xanthine oxidase, L-ascorbic acid, potassium superoxide and Hepes buffer were obtained from Sigma (St. Louis, MO, U.S.A.). $MnSO_4$ and phosphates for buffers were obtained from Fisher Scientific Co. (Fair Lawn, NJ, U.S.A.) and manganese(IV) oxide (MnO_2) was from Alfa Products (Ward Hill, MA, U.S.A.). H.p.l.c.-grade dimethyl sulphoxide (DMSO) was purchased from Aldrich (Milwaukee, WI, U.S.A.). Chelex 100 cation-exchange resin was purchased from Bio-Rad Laboratories (Richmond, CA, U.S.A.). Reagents were used without further purification. All reagent preparations and transfers were done using polyethylene or polypropylene labware to avoid possible undesirable trace-metal-ion contamination from glassware. Metal-free water was used in all solutions. This water was obtained by stirring (4–6 h; room temperature) Chelex 100 resin (1 %, w/v) with NANO-pure water obtained from a Sybron/Barnstead NANO-pure system. The water was then filtered using a 0.2 μm-pore-size disposable plastic filter and stored refrigerated for further use. Buffers were treated again with Chelex 100 resin and the pH was adjusted to 7.8 before use.

Solutions of SOD enzymes (0.01–100 nM) and manganese complexes (0.01–10 μM) were prepared in metal-free phosphate or Hepes buffers (5 mM, pH 7.8). The specific activity of SOD enzymes measured by the cytochrome *c* assay method was used to determine enzyme concentrations in solutions used in the kinetic experiments [1]. The green MnO_2–Desferal and pink MnO_2–Desferal–ascorbate complexes were synthesized as described elsewhere [31] and assayed in kinetic experiments the same day. $MnSO_4$ solutions were prepared in metal-free water and then diluted to the required concentration (0.01–10 μM) in buffer.

The spin trap DMPO obtained from Aldrich was shown to be free of radical impurities by e.s.r. before its use in competition experiments. DMPO concentrations were determined spectrophotometrically (wavelength 227 nm; $\epsilon = 8 \times 10^3\ M^{-1} \cdot cm^{-1}$) [38,39].

The kinetic experiments were done by adding O_2^- directly to buffered (pH 7.8) SOD, MnO_2–Desferal, MnO_2–Desferal–ascorbate or Mn^{2+} solutions containing DMPO (0.2 M). The final pH of reaction mixtures after completion of the experiments was pH 7.7 $\pm$ 0.1. Saturated O_2^- stock solutions were prepared by dissolving KO_2 in dry DMSO in capped plastic test tubes. The test tubes were fitted with a Teflon-covered syringe needle through which dry nitrogen gas was continuously bubbled to eliminate air and humidity above the solutions. In kinetic experiments, combined e.s.r. spectra of DMPO–O_2^-/DMPO–OH spin adducts recorded 30–45 s after addition of sufficient KO_2 to yield 20 μM-O_2^- in reaction mixtures. Each point in the kinetic plots represents an average of at least five separate determinations made with different enzyme or manganese preparations. Since it is known that DMPO–O_2^- decomposes forming DMPO–OH [17,38,40], the spectrometer modulation amplitude was increased to 1.0 mT in order to combine the e.s.r. spectra of the DMPO–O_2^- and DMPO–OH into a single e.s.r. spectrum. This procedure permits a more accurate measurement of the O_2^- trapped by DMPO. The O_2^- concentration in the KO_2 stock solution was measured by double integration of the first-derivative DMPO–O_2^- e.s.r. spectrum after addition of a known volume of KO_2 solution to 1.0 ml of DMSO containing DMPO (0.2 M). The stable free radical 3-carboxyproxyl was the concentration standard used to estimate that the KO_2 stock solution was 2 mM, based on spectral integration and a 91 % spin-trapping efficiency of O_2^- by DMPO in DMSO [41]. Spin-adduct concentrations in kinetic experiments were also determined by double integration of their first-derivative e.s.r. spectra. Furthermore, to avoid possible complications involving the presence of multiple spin adducts (DMPO–O_2^- and DMPO–OH) having different lifetimes in aqueous solutions, double integrations were carried out using the complete e.s.r. spectrum of the DMPO spin adducts. This was achieved by rapidly scanning the spectrum over a large scan range and using a high modulation amplitude. The e.s.r. spectrum obtained in this manner is virtually collapsed into a single peak.

After recording an e.s.r. spectrum for double integration, an e.s.r. spectrum of a separate identical reaction mixture was recorded with the spectrometer set for the kinetic experiments. This allows the peak-to-peak height of an individual e.s.r. line to be correlated with the concentration of DMPO spin adducts, since all e.s.r. spectra in the kinetic experiments were taken under identical conditions and no changes were observed in the e.s.r. linewidths. Hereafter, the low-field e.s.r. peak used to determine the total spin-adduct concentration present will be referred to as '[DMPO–O_2^-]'.

All e.s.r. spectra were recorded on a Varian E-109 X-band spectrometer at 100 kHz magnetic-field modulation. The magnetic field was set at 340.0 mT, microwave frequency at 9.510 GHz, microwave power at 10 mW and the time constant at 0.128 s. The instrument settings for kinetic experiments and for double integration respectively were: modulation amplitude: 1.0 mT and 4.0 mT; scan time: 2 min and 30 s; scan width: 10 mT and 50 mT. For Mn^{2+} e.s.r. spectra the magnetic field was set at 370.0 mT, microwave frequency at 9.510 GHz, microwave power at 10 mW, time constant at 0.25 s, scan time at 4 min and scan width at 200.0 mT.

The data generated by competition assays were analysed by assuming that a steady state was established during the reactions. The measured final concentration of DMPO–O_2^- spin adduct in the absence of dismutase, $[DMPO\text{–}O_2^-]_0$, is a function of the velocities of both the reaction of O_2^- with DMPO, spontaneous O_2^- dismutation at pH 7.8 (V_{SPON}; reactions 3 and 4), plus scavenging of O_2^- by DMPO–O_2^- and DMPO–OH spin adducts (V_{SA}):

$$[DMPO\text{–}O_2^-]_0 = f(V_{DMPO}, V_{SPON} \text{ and } V_{SA})$$

The measured final concentration of DMPO–O_2^- spin adduct in the presence of dismutase, $[DMPO–O_2^-]_c$, is a complex function:

$$[DMPO–O_2^-]_c = f(V_{DMPO}, V_{SPON}, V_{SA} \text{ and } V_{SOD})$$

Eqn. (B) can be derived from the steady-state model plus the fact that $[O_2^-] = K_m$ when the competition condition shown in eqn. (A) is satisfied [13–15]:

$$([DMPO–O_2^-]_0/[DMPO–O_2^-]_c) - 1 = k_{SOD}[SOD]/k_{DMPO}[DMPO] \quad (B)$$

The equation may be applied to the reaction mixtures used experimentally to determine the order with respect to SOD or dismutase [42].

Double-reciprocal plots of percentage inhibition as a function of dismutase concentration have been described [43–45]. Percentage inhibition for the reaction mixtures is:

$$100 \times \frac{[DMPO–O_2^-]_0 - [DMPO–O_2^-]_c}{[DMPO–O_2^-]_0}$$

$[DMPO–O_2^-]_0$ and $[DMPO–O_2^-]_c$ must be proportional to $[O_2^-]$, which varies inversely with the logarithm of the SOD concentration.

RESULTS

Although the reaction between O_2^- and DMPO initially generates the DMPO–O_2^- spin adduct (reaction 4), it is well known that this spin adduct has a half-life of about 35 s at pH 7.8, decomposing into products including DMPO–OH [17,39,40]. Therefore accurate measurement of O_2^- in an aqueous solution by spin trapping with DMPO is difficult, and care must be taken to develop a method which accounts for all the O_2^- that has reacted with DMPO. In most cases when O_2^- reacts with DMPO in an aqueous environment, a superimposition of the e.s.r. spectra corresponding to DMPO–O_2^- and DMPO–OH is observed. The e.s.r. spectra of these spin adducts have been well characterized, with hyperfine coupling constants $a_N = 1.41$ mT, $a_H = 1.13$ mT and $a_H = 0.125$ mT for DMPO–O_2^-, and, for DMPO–OH, $a_N = a_H = 1.49$ mT [46]. Fig. 1(*a*) shows the twelve-line DMPO–O_2^- e.s.r. spectrum superimposed on the typical DMPO–OH 1:2:2:1 quartet (marked by arrows) generated after addition of KO_2. A similar spectrum can be generated in 5 mM-Hepes buffer, pH 7.8. Since the DMPO–OH originates from the DMPO–O_2^- in an aqueous solution, a more accurate representation and measurement of the total amount of O_2^- reacting with DMPO will be a combination of the DMPO–O_2^- and DMPO–OH e.s.r. spectral intensities. Fig. 1(*b*) shows the e.s.r. spectrum obtained when the contributions from the DMPO–O_2^- and DMPO–OH e.s.r. peaks in Fig. 1(*a*) are combined into single peaks. This spectrum was generated after an increase in the instrument modulation amplitude from 0.05 mT (Fig. 1*a*) to 1.0 mT (Fig. 1*b*). Since the intensity of the e.s.r. signal is directly proportional to the concentration of the species being measured, double integration of the first-derivative spectrum in Fig. 1(*b*) allows determination of the total concentration of spin adducts originating from the reaction between O_2^- and DMPO. This type of e.s.r. measurement is essential in studies involving competition-kinetic reactions using O_2^- and DMPO.

The spectrum in Fig. 1(*b*) represents a combination of the e.s.r. spectra of DMPO–O_2^- and DMPO–OH spin adducts, each of which has a different stability. The combined e.s.r. spectrum's decay rate was examined to determine whether kinetic measurements could be made after O_2^- addition. Fig. 2(*a*) shows that the decay with time of the low-field e.s.r. peak in Fig. 1(*b*) was relatively small over a 3 min time period; 30 s were required to start the e.s.r. measurement after O_2^- addition. All kinetic experiments measured the e.s.r. signal 30 to 45 s after O_2^- addition (arrows) to take advantage of the relatively modest change in signal intensity over that time span.

On the basis of preliminary empirical results, a 0.2 M-DMPO concentration was chosen for reaction mixtures. The optimal initial O_2^- concentration was then determined which satisfied two experimental criteria. First, the resultant e.s.r. signal from the chosen O_2^- concentration in 0.2 M-DMPO had to be large

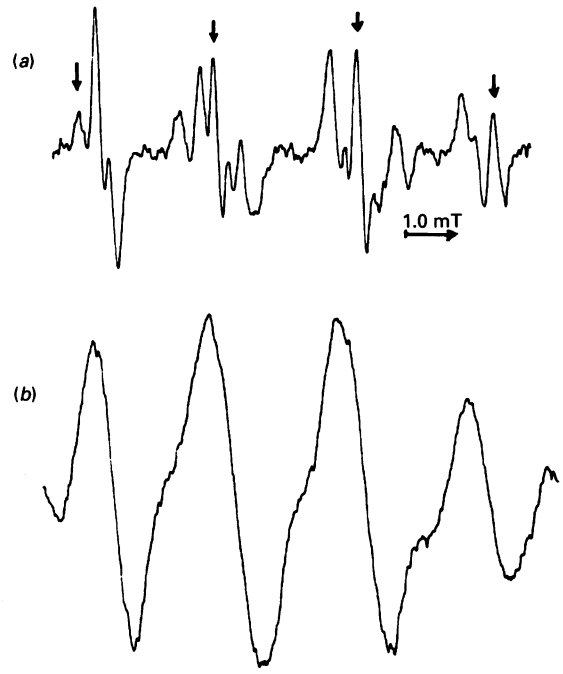

Fig. 1. E.s.r. spectra of DMPO adducts after O_2^- addition

(*a*) An e.s.r. spectrum of DMPO–O_2^- and DMPO–OH adducts at an instrument modulation amplitude of 0.05 mT. Other instrument settings are listed in the Experimental section. The DMPO–OH 1:2:2:1 quartet is marked by arrows in the combined DMPO–O_2^- and DMPO–OH spectrum. (*b*) An e.s.r. spectrum of a solution identical with the one used in (*a*) with the same instrument settings, except the instrument modulation amplitude was changed to 1.0 mT.

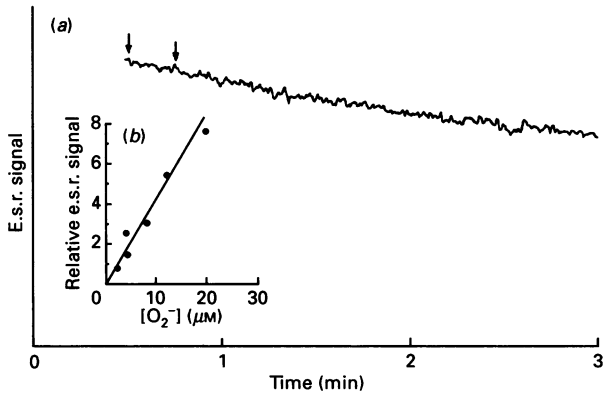

Fig. 2. E.s.r. spectral responses

(*a*) Reduction of the combined DMPO–O_2^- and DMPO–OH adducts with time. The instrument magnetic field was locked on the low-field e.s.r. peak in Fig. 1(*b*) and the scan range was set to zero. Measurement began 30 s after O_2^- addition to the reaction mixture. Inset (*b*): relative e.s.r. signal intensity as a function of O_2^- concentration. Instrument settings were those for kinetic experiments in the Experimental section.

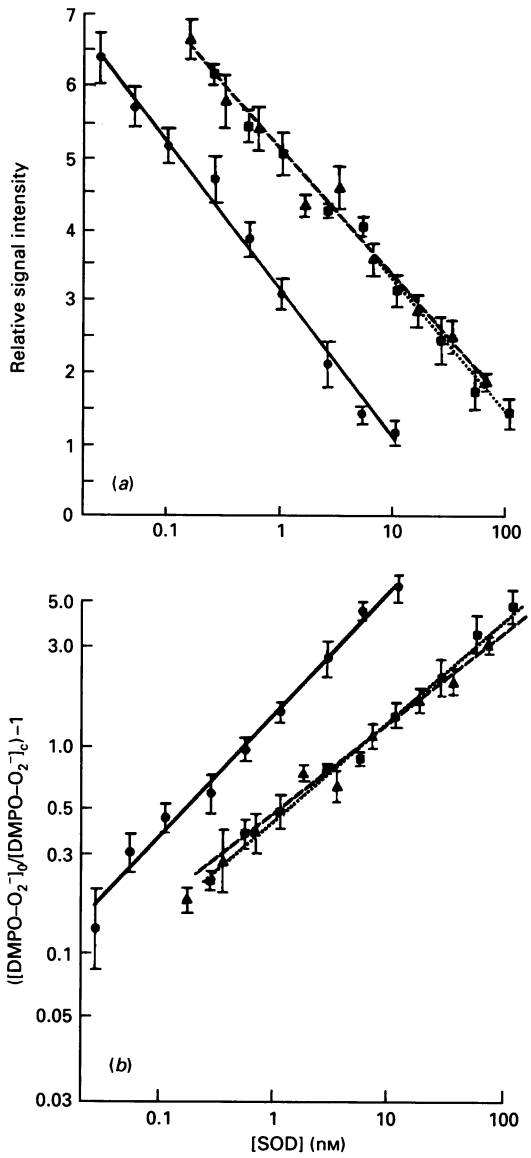

Fig. 3. DMPO–O_2^- spin-adduct formation

(*a*): ●, Spin-adduct formation at increasing [Cu,Zn-SOD]; ▲, at increasing [Mn-SOD]; ■, at increasing [Fe-SOD]. Bars represent the S.E.M. for each value. The straight-line correlation coefficients are −0.95 for Cu,Zn-SOD, −0.95 for Fe-SOD and −0.93 for Mn-SOD data. (*b*) Graphical representations of the logarithm of the overall reaction velocities, $([DMPO–O_2^-]_0/[DMPO–O_2^-]_c)-1$, as a function of log[SOD]. ●, Cu,Zn-SOD; ▲, Mn-SOD; ■, Fe-SOD. Bars represent the S.E.M. at each value. Cu,Zn-SOD data have a straight-line correlation coefficient of 0.95, Fe-SOD has a value of 0.93, and Mn-SOD has a value of 0.95.

Table 1. ID_{50} values for SOD species, Mn^{2+} standard and Mn^{2+} complexes

The ID_{50} values for either SOD enzyme or Mn^{2+} were determined by the analytical methods shown; 95% confidence intervals are shown in brackets. The Mn^{2+} standard was prepared from $MnSO_4$. Mn^{2+} in complexes was measured by e.s.r. and adjusted to concentrations equal to those of the standards.

	ID_{50} (M)	
Graphical method of determination... Compound	$[DMPO–O_2^-]_c$ versus log (concn.)	1/Percentage inhibition versus $1/[SOD]^{0.5}$ or $1/[Mn^{2+}]$
Cu,Zn-SOD	$0.53\ [0.44, 0.64]\times10^{-9}$	$0.59\ [0.35, 0.83]\times10^{-9}$
Fe-SOD	$5.5\ [4.6, 6.6]\times10^{-9}$	$5.4\ [4.0, 6.8]\times10^{-9}$
Mn-SOD	$5.9\ [4.7, 7.6]\times10^{-9}$	$4.7\ [3.0, 6.4]\times10^{-9}$
Mn^{2+} standard	$1.4\ [1.1, 1.5]\times10^{-6}$	$1.7\ [-0.70, 4.1]\times10^{-6}$
Mn^{2+} complexes	$1.2\ [1.0, 2.0]\times10^{-6}$	$1.3\ [0.71, 1.9]\times10^{-6}$

enough to be conveniently measured. Secondly, the initial O_2^- concentration selected had to be in the linear response range for e.s.r. signal intensity as a function of O_2^- concentration. Fig. 2(*b*) shows results obtained after the addition of increasing O_2^- concentrations to 0.2 M-DMPO in 5 mM-phosphate buffer, pH 7.8. There is an apparently linear relationship between the e.s.r. relative signal intensity and $[O_2^-]$ up to 20 μM under the assay conditions described. There was a loss of linear response above 20 μM-O_2^- in our reaction mixtures. About 50% of the 20 μM initial O_2^- concentration was trapped by 0.2 M-DMPO in reaction mixtures, with the remainder being lost through spontaneous dismutation (reaction 3). Therefore, a 20 μM-O_2^- initial concentration was selected for kinetic assays because it best satisfied both the above experimental criteria.

The relative e.s.r. signal was measured at increasing SOD concentrations in reaction mixtures with 5 mM-phosphate buffer, pH 7.8, 0.2 M-DMPO, and initial O_2^- concentrations of 20 μM. Fig. 3(*a*) shows the linear correlation between DMPO spin adducts formed and log[SOD] for each enzyme. The linear relationship is maintained over two logarithmic cycles of SOD concentration. At enzyme concentrations above or below those shown, the linear relationship is not followed. There is no significant difference between Fe-SOD and Mn-SOD ($P > 0.1$), but the slope of the Cu,Zn-SOD line differs from the slopes of lines for each of the other enzymes ($P < 0.05$). The ID values are shown in Table 1.

The data generated in the reaction mixtures can be analysed to determine the order of SOD in the overall reaction [42]. Plots of the $\log([DMPO–O_2^-]_0/[DMPO–O_2^-]_c)-1$ versus log[SOD] (eqn. B) are shown in Fig. 3(*b*). The Cu,Zn-SOD line has a slope of 0.59, Fe-SOD data have a slope of 0.48, and Mn-SOD has a slope of 0.44. The average of the slopes for all three enzymes is 0.5. This unexpected result indicates that, in these competition assays, SOD acts as if it were a half-order molecular species.

The slope of approx. 0.5 for enzymes in Fig. 3(*b*) indicates that the data would be curvilinear on a linear scale, increasing rapidly at low enzyme concentrations and levelling off at higher enzyme concentrations. In addition to an apparent half-order reaction to explain the data, there are two other possible reasons for the curvilinear direct plot. It is possible that H_2O_2 causes reversibility of reaction (2) at higher enzyme concentrations. More O_2^- could be generated and trapped by DMPO, resulting in a smaller value for $[DMPO–O_2^-]_0/[DMPO–O_2^-]_c$. Furthermore, it has recently been proposed that H_2O_2 reacts with SOD yielding hydroxyl radicals, which could also be trapped by DMPO, yielding a lower-than-expected $[DMPO–O_2^-]_0/[DMPO–O_2^-]_c$ ratio [47]. In order to determine the effect of H_2O_2 on the DMPO-spin-adduct e.s.r. spectra, the H_2O_2 formed in reaction mixtures was removed by addition of 500 units of catalase/ml before O_2^- addition. A second series of control experiments incorporated a fivefold excess of H_2O_2 (50 μM) in reaction mixtures before O_2^- addition. Neither removal of H_2O_2 by catalase nor prior enhancement of the H_2O_2 concentration had an effect on the DMPO-spin-adduct e.s.r. spectra. Another possible factor at low enzyme concentrations could be reaction of O_2^- with DMPO–O_2^-

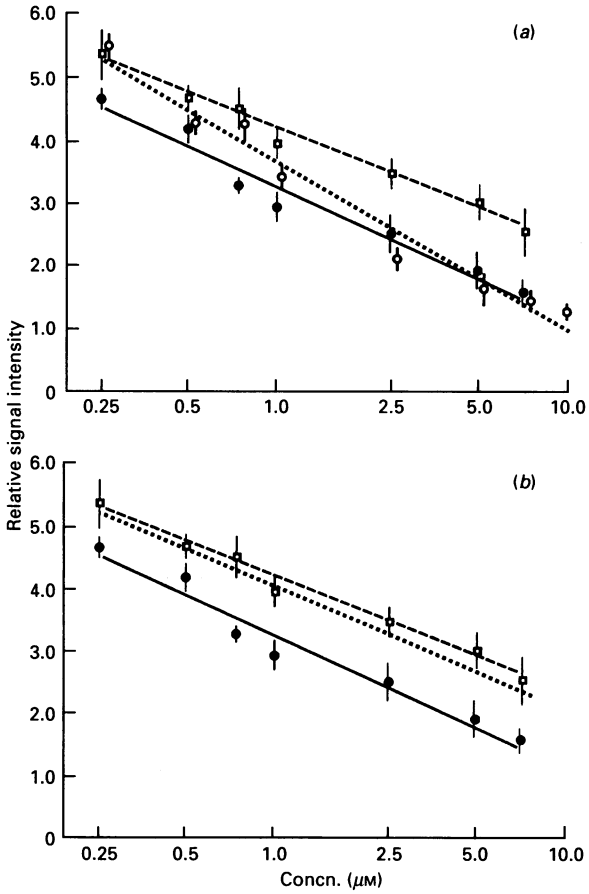

Fig. 4. DMPO–O_2^- spin-adduct formation

(*a*) Spin adduct formation: ●, at increasing [$MnSO_4$]; □, at increasing MnO_2–Desferal; ○, at increasing [MnO_2–Desferal – ascorbate]. The straight-line correlation coefficients are −0.91 for $MnSO_4$, −0.84 for MnO_2–Desferal and −0.95 for MnO_2–Desferal–ascorbate. (*b*) Spin-adduct formation for $MnSO_4$ (●), MnO_2–Desferal (□) and MnO_2–Desferal–ascorbate corrected for ascorbate (·····).

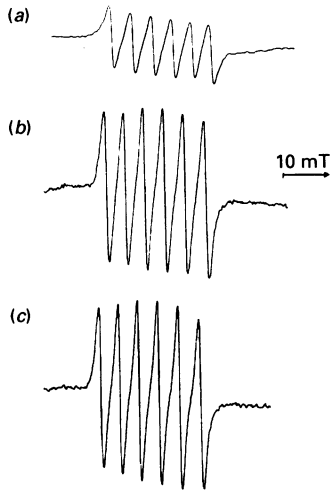

Fig. 5. E.s.r. spectra of 0.1 mM-$MnSO_4$ in three solvents

(*a*) 5 mM-Phosphate buffer, pH 7.8; (*b*) solution in (*a*) acidified below pH 5.5; (*c*) 5 mM-Hepes buffer, pH 7.8.

or DMPO–OH spin adducts [20,21]. However, at low enzyme concentrations the relative e.s.r. signal intensity decreased linearly, indicating that scavenging of O_2^- by the spin adducts is unimportant. Since H_2O_2 or reaction of O_2^- with DMPO–O_2^- and DMPO–OH appear to have no effect on the results, the most likely explanation is an apparent half-order process.

The data in Fig. 3(*a*) were analysed by double-reciprocal plots of percentage inhibition versus [SOD]. These data only approximate straight lines as the SOD concentrations varied. Double-reciprocal plots of percentage inhibition as a function of $[SOD]^{0.5}$ more closely fit a straight line for each enzyme. The straight-line correlation coefficients and ordinate intercepts for Cu,Zn-SOD, Mn-SOD and Fe-SOD were, respectively, 0.82, 0.89 and 0.88, and 1.11 and 0.93 and 1.03.

The relative e.s.r. signal was measured at increasing manganese, MnO_2–Desferal or MnO_2–Desferal–ascorbate concentrations in 5 mM-phosphate buffer, pH 7.8, as described for SOD above. Fig. 4(*a*) indicates the linear relationship between DMPO spin adducts formed and the logarithm of the concentration for each preparation. The slope of the MnO_2–Desferal–ascorbate line indicated a possible contribution to reduction of the e.s.r. signal by increasing ascorbate at higher concentrations. Ascorbate was measured at the concentrations used to generate data in Fig. 4(*a*), and the point-by-point correction resulted in the data shown in Fig. 4(*b*). The MnO_2–Desferal–ascorbate preparation corrected for ascorbate yields results similar to the MnO_2–Desferal preparation. Moreover, both Desferal preparations were different from the Mn^{2+} standard, which appeared more active by a factor of 3 as an O_2^- scavenger. ID_{50} values were 0.58×10^{-6} M for Mn^{2+}, 1.7×10^{-6} M for MnO_2–Desferal and 1.4×10^{-6} M for MnO_2–Desferal–ascorbate.

A 5 mM-potassium phosphate buffer, pH 7.8, was used for SOD enzyme experiments described above. However, it is known that Mn^{2+} forms hydroxides or phosphates at basic pH. The e.s.r. spectra were obtained of 0.1 mM-$MnSO_4$ samples in different solvents, and the results are shown in Fig. 5. The Mn^{2+} e.s.r. spectrum was present in each solution, but 5 mM-phosphate buffer, pH 7.8, clearly decreased the relative signal intensity. The relative e.s.r. signal intensity was equal for Mn^{2+} in acidified phosphate or 5 mM-Hepes, pH 7.8. The e.s.r. signal intensity observed in Fig. 5(*b*) represents total Mn^{2+} present in solution. Since the intensity of e.s.r. signals shown in Figs. 5(*b*) and 5(*c*) are equal, the results suggest that Hepes buffer stabilizes total free Mn^{2+} sufficiently to allow quantification. Results similar to those in Fig. 5 were obtained for each complex in Hepes and phosphate buffer at pH 7.8.

Kinetic experiments were done with $MnSO_4$ standards, MnO_2–Desferal complex and MnO_2–Desferal–ascorbate complexes in 5 mM-Hepes, pH 7.8. The concentrations of Mn^{2+} in each of the complexes were adjusted to equal the Mn^{2+} concentration measured by e.s.r. in standards prepared from $MnSO_4$. This procedure ensures different concentrations of $MnSO_4$, MnO_2–Desferal complex and MnO_2–Desferal–ascorbate complex. However, the free Mn^{2+} concentration is nearly equal in each preparation. Fig. 6(*a*) shows the results of these kinetic determinations. There appears to be a correlation between the relative e.s.r. signal and the logarithm of the Mn^{2+} concentration over nearly two logarithmic cycles. There was a decrease in the e.s.r. relative signal intensity in the absence of dismutase in 5 mM-Hepes, pH 7.8, compared with 5 mM-phosphate, pH 7.8, from 7.6 to 5.4 units. The decrease may reflect a reaction of O_2^- with 5 mM-Hepes and was considered equal in each solution. There appears to be a slight difference in the slopes of MnO_2–Desferal–ascorbate lines compared with either Mn^{2+} or MnO_2–Desferal. The presence of ascorbate probably accounts for this difference. However, statistically there is no difference ($P > 0.1$) between

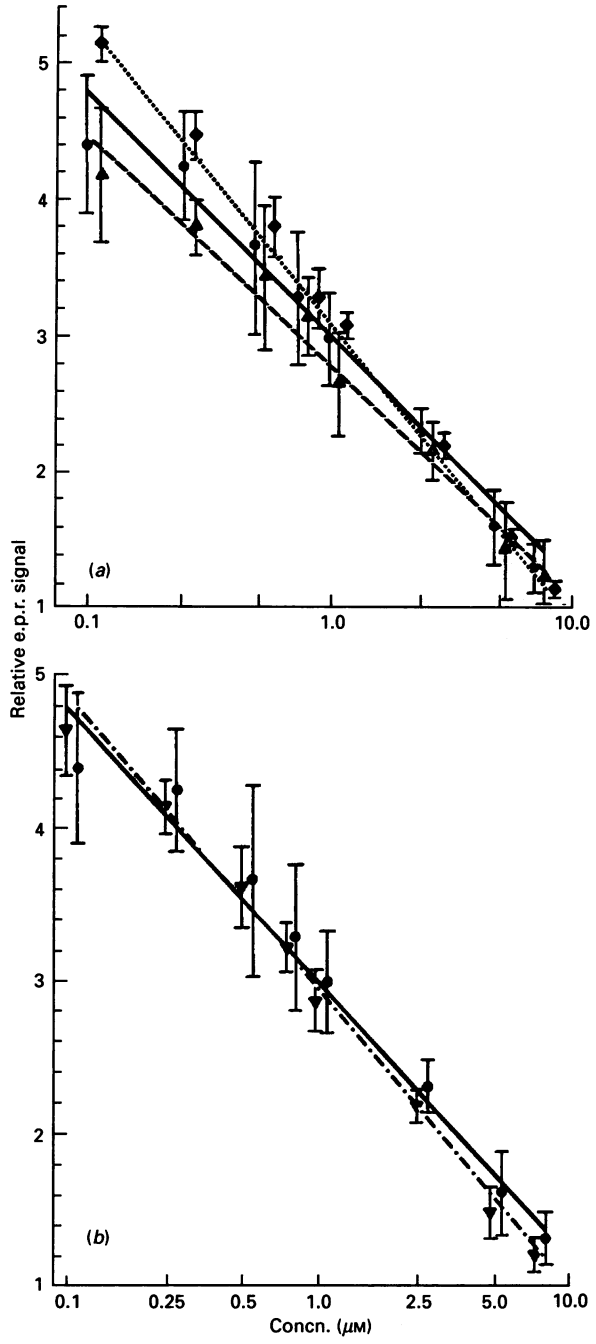

Fig. 6. DMPO spin-adduct formation for Mn^{2+} and complexes

(*a*) Spin-adduct formation: ●, at increasing [Mn^{2+}]; ▲, at increasing [MnO_2–Desferal complex]; ◆, at increasing [MnO_2–Desferal–ascorbate]. (*b*) Spin-adduct formation: ●, at increasing [Mn^{2+}]; ▼, data for the MnO_2–Desferal and MnO_2–Desferal–ascorbate were combined. The straight-line correlation coefficients are −0.91 for $MnSO_4$ standards and −0.83 for the combined-complex data.

each of the slopes of the three lines, suggesting that dismutase activity in solutions of the two Mn^{2+} complexes resides in Mn^{2+}. Fig. 6(*b*) shows results from kinetic experiments comparing combined MnO_2–Desferal and MnO_2–Desferal–ascorbate-complex data with data for the $MnSO_4$ standard. The probability that the lines differ is $P > 0.1$. The calculated ID_{50} for each of the lines is listed in Table 1.

The data for Mn^{2+} in $MnSO_4$ standards and Mn^{2+} for the combined complexes were analysed by double-reciprocal plots of

Table 2. Second-order rate constants for SOD species and Mn^{2+}

Rate constants for O_2^- reaction with SOD enzymes and Mn^{2+} were estimated. Determinations were made from average ID_{50} values from Table 1 on the basis of the equality expression (A) (see the text). The 95% confidence intervals are shown in square brackets.

Compound	Rate constant ($M \cdot s^{-1}$)
Cu,Zn-SOD	$6.4\,[4.9, 7.9] \times 10^9$
Fe-SOD	$6.6\,[5.5, 7.7] \times 10^8$
Mn-SOD	$6.8\,[5.4, 8.2] \times 10^8$
Mn^{2+} standard	$2.3\,[0.46, 4.1] \times 10^6$
Mn^{2+} complexes	$2.9\,[2.2, 3.6] \times 10^6$

percentage inhibition versus [Mn^{2+}]. Linear plots were generated and ID_{50} values estimated at the 50%-inhibition point (Table 1). Further, data from Table 1 were used to calculate velocity constants shown in Table 2.

DISCUSSION

The observation that the DMPO–O_2^- spin adduct e.s.r. signal is inversely proportional to log[SOD] for each of the three enzymes tested supports the validity of this competition assay. A similar result was reported for Cu,Zn-SOD using DMPO as a spin trap and a xanthine–xanthine oxidase O_2^- generator [19]. A number of studies based on competition assays for SOD activity indicate that inhibition of the reaction of O_2^- with detector molecule is a function of log[SOD] [43–45]. Therefore it is reasonable to conclude that the measured DMPO–O_2^- spin adduct e.s.r. signal is a function of the O_2^- concentration, which in turn depends on log[SOD]. In the above experiments, the rate of spontaneous O_2^- dismutation or reaction of O_2^- with the DMPO–O_2^- and DMPO–OH adducts formed was ineffective in masking the enzymic contribution to O_2^- removal over the linear ranges of the assays.

The unexpected finding that competition reaction mixtures are apparently half-order with respect to SOD may be explained if steady-state conditions are present. Redox cycling of SOD occurs when $[O_2^-] \gg [SOD]$, establishing conditions where both the M^{n+}–SOD and $M^{(n-1)+}$–SOD forms of the enzyme compete against DMPO for O_2^- (reactions 1 and 2). Also, fast-kinetic results have shown that, under less-than-saturating O_2^- concentrations, the rate-limiting step for the Cu,Zn-SOD and Fe-SOD enzymes is reaction with O_2^- [11,12]. Reactions (1) and (2) may then be represented as the following steady-state expression:

$$M^{n+}\text{–SOD} + O_2^- \underset{k_{-1}}{\overset{k_{+1}}{\rightleftharpoons}} O_2 + M^{(n-1)+}\text{–SOD}$$

$$+ O_2^- + 2H^+ \underset{k_{-2}}{\overset{k_{+2}}{\rightleftharpoons}} H_2O_2 + M^{n+}\text{–SOD}$$

In this case, $k_{-2} \ll k_2$, M^{n+}–SOD–O_2^- and $M^{(n-1)+}$–SOD–O_2H_2 are comparatively small, and the steady-state intermediate is $M^{(n-1)+}$–SOD. Starting with the expression $k_{+1}[O_2^-][M^{n+}\text{–SOD}] = (k_{+2}+k_{-1})[M^{(n-1)+}\text{–SOD}]$, it can be shown that:

$$[M^{n+}\text{–SOD}][O_2^-]/[M^{(n-1)+}\text{–SOD}] = (k_{+2}+k_{-1})/k_{+1} = K_m$$

If SOD is defined as the total concentration of enzyme in all forms, then the following expression results:

$$(\text{SOD} - [M^{(n-1)+}\text{–SOD}])[O_2^-]/[M^{(n-1)+}\text{–SOD}] = K_m$$

Rearrangement results in an expression similar to the Briggs–Haldane equation [48]:

$$[M^{(n-1)+}\text{–SOD}] = \text{SOD}\,[O_2^-]/([O_2^-]+K_m)$$

At half-maximal velocity, by definition, $[O_2^-] = K_m$. This necessary condition for steady-state kinetics substituted into the equation analogous to the Briggs–Haldane expression yields the result $[M^{(n-1)+}\text{–SOD}] = 0.5\,\text{SOD}$ with $[M^{(n-1)+}\text{–SOD}] \approx [M^{n+}\text{–SOD}]$. Therefore competition reactions between DMPO and nearly equal concentrations of M^{n+}–SOD and $M^{(n-1)+}$–SOD for O_2^- result in an apparent half-order with respect to SOD. It must be stressed that this apparent half-order applies specifically to competition reactions when $[O_2^-] \gg [\text{SOD}]$. Often a low steady state $[O_2^-]$ generated enzymically and higher SOD concentrations are employed to estimate dismutase levels [1–3,15,19].

There are limitations imposed when attempting to assay O_2^- dismutation using a competition method. One important factor is accuracy of the value of k_{DMPO} for estimates of k_{SOD}. The value $k_{DMPO} = 18\ M^{-1}\cdot s^{-1}$ was used in the present study, but there is considerable variation reported for this rate constant [18,49]. The accuracy of values for k_{SOD} reported above will be directly related to the accuracy of the k_{DMPO} value chosen for calculation. In addition, second-order rate constants determined from average ID_{50} values are higher than many previous determinations [7,11,12,22,50]. Elevated k_{SOD} values in Table 2 are probably based on median ID_{50} values that are too low. Spontaneous dismutation plus O_2^- reaction with DMPO–O_2^- or DMPO–OH spin adducts may be causing underestimation of ID_{50} values and overestimation of velocity constants in the present study.

The competition between DMPO and Mn^{2+} for O_2^- occurs in the micromolar Mn^{2+} concentration range. Relatively high Mn^{2+} concentrations are required because the reaction rate constant of O_2^- with Mn^{2+} is much lower than k_{SOD} in eqn. (A). The increased Mn^{2+} concentration required approaches the 20 μM-O_2^- concentration initially present in reaction mixtures. This relative reduction in the ratio of O_2^- to Mn^{2+} compared with the higher analogous ratio with the SOD enzymes may result in a simple chemical reaction between Mn^{2+} and O_2^- rather than a dismutation reaction. Mn^{2+} competition with DMPO using these limiting O_2^- concentrations would not permit steady-state redox cycling of Mn^{2+} in competition assays.

An additional major finding of the present study is that the SOD activity of the MnO_2–Desferal and MnO_2–Desferal–ascorbate complexes is correlated with the Mn^{2+} concentration present in the preparations. Since Mn^{2+} is always present in either the MnO_2–Desferal or the MnO_2–Desferal–ascorbate complexes, it is not possible to demonstrate SOD activity uniquely attributable to either complex or Mn^{2+} in any of the preparations. The possibility exists that SOD activity in complex preparations is due to Mn^{2+}, complex, a combination of both free Mn^{2+} and complex, or additional manganese species acting alone or in combination with any or all of the above materials [31]. Nevertheless, the observation of equivalent SOD activity for $MnSO_4$ standards and manganese-complex preparations adjusted to concentrations of Mn^{2+} equal to those of standards strongly supports the contention that O_2^- removal by complexes is due to Mn^{2+}.

This work was supported by the Armed Forces Radiobiology Research Institute (AFRRI), Defense Nuclear Agency, under work unit 00162/00150. Views presented in this paper are those of the authors; no endorsement by the Defense Nuclear Agency has been given or should be inferred. Research was conducted according to the principles enunciated in the 'Guide for the Care and Use of Laboratory Animals' prepared by the Institute of Laboratory Animal Resources, National Research Council. We are very grateful to Mr. William Jackson for statistical analysis of the data in this paper. We also thank Mrs. Betty Gray for preparing this manuscript, the AFRRI visual media division for preparing the Figures and Mr. Troy S. Kimmel for preparation of Tables.

REFERENCES

1. McCord, J. M. & Fridovich, I. (1969) J. Biol. Chem. **244**, 6049–6055
2. Keele, B. B., Jr., McCord, J. M. & Fridovich, I. (1970) J. Biol. Chem. **245**, 6176–6181
3. Yost, F. J., Jr. & Fridovich, I. (1973) J. Biol. Chem. **248**, 4905–4908
4. Dougherty, H. W., Sadowski, S. J. & Baker, E. E. (1978) J. Biol. Chem. **253**, 5220–5223
5. Steinman, H. M. (1982) in Superoxide Dismutase (Oberley, L. W., ed.), vol 1, pp. 11–68, CRC Press, Boca Raton, FL
6. Fridovich, I. (1986) Ad. Enzymol. Relat. Areas Mol. Biol. **58**, 61–97
7. Klug, D., Rabani, J. & Fridovich, I. (1972) J. Biol. Chem. **247**, 4839–4842
8. Pick, M., Rabani, J., Yost, F. & Fridovich, I. (1974) J. Am. Chem. Soc. **96**, 7329–7333
9. Lavelle, F., McAdam, M. E., Fielden, E. M., Roberts, P. B., Puget, K. & Michelson, M. (1977) Biochem. J. **161**, 3–11
10. Osman, R. & Basch, H. (1984) J. Am. Chem. Soc. **106**, 5710–5714
11. Bull, C. & Fee, J. A. (1985) J. Am. Chem. Soc. **107**, 3295–3304
12. Fee, J. A. & Bull, C. (1986) J. Biol. Chem. **261**, 13000–13005
13. Michaelis, L. & Menten, M. L. (1913) Biochem. Z. **49**, 333–369
14. Adams, G. E., Boag, J. W., Currant, J. & Michael, B. D. (1965) in Pulse Radiolysis (Ebert, M., Keene, J. P., Swallow, A. J. & Baxendale, J. H., eds.), pp. 131–143, Academic Press, New York
15. Bors, W., Michel, C. & Saran, M. (1985) in CRC Handbook of Methods for Oxygen Radical Research (Greenwald, R. A., ed.), pp. 181–188, CRC Press, Boca Raton, FL
16. Behar, D., Czapski, G., Rabani, J., Dorfman, L. M. & Schwarz, H. A. (1970) J. Phys. Chem. **74**, 3209–3213
17. Harbour, J. R., Chow, V. & Bolton, J. R. (1974) Can. J. Chem. **52**, 3549–3553
18. Finkelstein, E., Rosen, G. M. & Rauckman, E. J. (1980) J. Am. Chem. Soc. **102**, 4994–4999
19. Mitsuta, K., Mizuta, Y., Kohno, M., Hiramatsu, M. & Mori, A. (1990) Bull. Chem. Soc. Jpn. **63**, 187–191
20. Samuni, A., Murali Krisna, C., Riesz, P., Finkelstein, E. & Russo, A. (1989) Free Radicals Biol. Med. **6**, 141–148
21. Buettner, G. R. (1990) Free Radicals Res. Commun. **10**, 11–15
22. Forman, H. J. & Fridovich, I. (1973) Arch. Biochem. Biophys. **158**, 396–400
23. Rabani, J., Klug, D. & Lilie, J. (1973) J. Phys. Chem. **77**, 1169–1175
24. Weinstein, J. & Bielski, B. H. J. (1980) J. Am. Chem. Soc. **102**, 4916–4919
25. Lengfelder, E. & Weser, U. (1981) Bull. Eur. Physiopathol. Respir. **17**, 73–80
26. Darr, D., Zarilla, K. A. & Fridovich, I. (1987) Arch. Biochem. Biophys. **258**, 351–355
27. Kubota, S. & Yang, J. T. (1984) Proc. Natl. Acad. Sci. U.S.A. **81**, 3283–3286
28. Samuni, A., Krishna, C. M., Riesz, P., Finkelstein, E. & Russo, A. (1988) J. Biol. Chem. **263**, 17921–17924
29. Rabinowitch, H. D., Privalle, C. T. & Fridovich, I. (1987) Free Radicals Biol. Med. **3**, 125–131
30. Rabinowitch, H. D., Rosen, G. M. & Fridovich, I. (1989) Free Radicals Biol. Med. **6**, 45–48
31. Beyer, W. F., Jr. & Fridovich, I. (1989) Arch. Biochem. Biophys. **271**, 149–156
32. Archibald, F. S. & Fridovich, I. (1982) Arch. Biochem. Biophys. **214**, 452–463
33. Goldstein, S., Michel, C., Bors, W., Saran, M. & Czapski, G. (1988) Free Radicals Biol. Med. **4**, 295–303
34. Ilan, Y., Ilan, Y. A. & Czapski, G. (1978) Biochem. Biophys. Acta **503**, 399–401
35. Marcus, R. A. & Sutin, N. (1985) Biochem. Biophys. Acta **811**, 2265–2322
36. Augustin, M. A. & Yandell, J. K. (1979) Inorg. Chem. **18**, 577–583
37. Koppenol, W. H., Levine, F., Hatmaker, T. L., Epp, J. & Rush, D. L. (1986) Arch. Biochem. Biophys. **251**, 594–599
38. Buettner, G. R. & Oberley, I. W. (1978) Biochem. Biophys. Res. Commun. **83**, 69–74
39. Kalyanaraman, B., Felix, C. C. & Sealy, R. C. (1982) Photochem. Photobiol. **36**, 5–12
40. Finkelstein, E., Rosen, G. M. & Rauchkman, E. J. (1979) J. Mol. Pharmacol. **16**, 676–685

41. Carmichael, A. J., Samuni, A. & Riesz, P. (1985) Photochem. Photobiol. **41**, 635–642
42. Cornish-Bowden, A. (1976) Principles of Enzyme Kinetics, p. 4, Butterworth and Co., London
43. Kobayashi, Y., Okahata, S., Tanabe, K. & Usui, T. (1978) J. Immunol. Methods **24**, 75–78
44. Eldred, G. E. & Hoffert, J. R. (1981) Anal. Biochem. **110**, 137–143
45. Sun, Y., Oberley, L. & Li, Y. (1988) Clin. Chem. **34**, 497–500
46. Buettner, G. R. (1987) Free Radicals Biol. Med. **3**, 259–303
47. Yim, M. B., Chock, P. B. & Stadtman, E. R. (1990) Proc. Natl. Acad. Sci. U.S.A. **87**, 5006–5010
48. Briggs, G. E. & Haldane, J. B. S. (1925) Biochem. J. **19**, 338–339
49. Yamazaki, I., Piette, L. H. & Grover, T. A. (1990) J. Biol. Chem. **265**, 652–659
50. Rabani, J., Klug, D. & Fridovich, I. (1972) Isr. J. Chem. **10**, 1095–1106

Received 7 May 1991/24 July 1991; accepted 5 August 1991